Review

Evaluation of Pharmacokinetic Drug–Drug Interactions: A Review of the Mechanisms, In Vitro and In Silico Approaches

Yaru Peng [ID]**, Zeneng Cheng and Feifan Xie ***

Division of Biopharmaceutics and Pharmacokinetics, Xiangya School of Pharmaceutical Sciences,
Central South University, Changsha 410013, China; yaru.peng@hotmail.com (Y.P.); chengzn@csu.edu.cn (Z.C.)
* Correspondence: feifan.xie@csu.edu.cn; Tel.: +86-0731-8265-0446

Abstract: Pharmacokinetic drug–drug interactions (DDIs) occur when a drug alters the absorption, transport, distribution, metabolism or excretion of a co-administered agent. The occurrence of pharmacokinetic DDIs may result in the increase or the decrease of drug concentrations, which can significantly affect the drug efficacy and safety in patients. Enzyme-mediated DDIs are of primary concern, while the transporter-mediated DDIs are less understood but also important. In this review, we presented an overview of the different mechanisms leading to DDIs, the in vitro experimental tools for capturing the factors affecting DDIs, and in silico methods for quantitative predictions of DDIs. We also emphasized the power and strategy of physiologically based pharmacokinetic (PBPK) models for the assessment of DDIs, which can integrate relevant in vitro data to simulate potential drug interaction in vivo. Lastly, we pointed out the future directions and challenges for the evaluation of pharmacokinetic DDIs.

Keywords: drug–drug interactions; pharmacokinetics; physiologically based pharmacokinetic model; cytochrome P450; transporter

1. Introduction

Drug–drug interactions (DDIs) can occur in patients undergoing polytherapy at pharmacokinetic (PK) and pharmacodynamic (PD) level, resulting in altered drug concentrations by either inhibiting or inducing the enzymes or transporters responsible for the disposition of that drug or producing agonistic or antagonistic effects [1]. Both the PK and PD interactions may lead to reduced efficacy or increased toxicity in the clinic. Compared to PD DDIs, which need a case-by-case evaluation [2,3], PK DDIs are more common and have received great attention from drug agencies [4,5]. Early termination of development, refusal of regulatory approval, and market withdrawals due to PK DDIs have been widely reported [6,7]. For example, in 1997, the US Food and Drug Administration (FDA) recalled the first non-sedating antihistamine-terfenadine due to its potential to reach lethal blood exposing levels when co-administered with some antibiotics like erythromycin and ketoconazole [8].

To mitigate the risk of costly developmental failure or undesired therapeutic outcomes, evaluation of DDIs has been integrated into the drug discovery stage and post-marketing administration. Traditionally, if in vitro studies indicate a high-risk for PK-related DDIs, a mechanistic static model will be applied, estimating the ratios of concentration area under the curve (AUCi/AUC) for cytochromes P450 (CYPs)- and transporter-based inhibition or induction in the presence (AUCi) or absence (AUC) of the perpetrator. However, most static models tend to overpredict the extent of DDIs since they are usually based on the maximum concentration of perpetrating drugs. Moreover, the static model approach assumes the same precipitant concentration, CYPs, and transporter expression levels across the population; thus, it only provides average estimates of the DDIs and the risk to individuals is not evaluated [9].

In recent years, physiologically based pharmacokinetic (PBPK) modeling is widely adopted by the pharmaceutical industry for DDIs evaluation because of its superior power to bridge in vitro and in vivo DDIs studies and the ability to predict complex DDIs in patient populations with various administration schemes [10–13]. As a mechanistic dynamic model, the PBPK approach is highly appreciated by the agencies for new drug applications and is gradually replacing the empirical static methods. CYPs hold a central position for DDIs studies since they account for the metabolism of about 45% of the marketed drugs [14]. Currently, the in vitro assays and in vitro-in vivo extrapolation (IVIVE) methods for CYPs meditated DDIs are quite mature and extensively reported [15–17]. Besides the CYPs-DDIs, the DDIs are caused by non-CYP enzymes and transporters, such as UDP-glucuronosyltransferases (UGTs), uptake transporters (OATPs, OATs, and OCTs) and efflux transporters (*P-gp*, BCRP), are also important but are poorly studied and less understood [18,19]. The power of PBPK modeling for transporters mediated DDIs is obvious, and some excellent cases for the OATPs transporter have been reported [20–22], and some new sights have been emerged for *P-gp* and BCRP recently [23–25]. To our knowledge, the static and dynamic models towards CYPs-DDIs are well reviewed [1,9,18,26], while a comprehensive summary of the static and dynamic models for both CYPs- and transporters-DDIs are scarce.

In this review, we provide an overview of the in vitro tools, conventional static approaches, and dynamic models for PK DDIs, where the CYPs and transporter-meditated inhibition or induction are covered. In addition, the limitations of these methodologies and future perspectives for handling PK-related DDIs are discussed.

2. Mechanisms for CYPs/Transporter-Mediated PK DDIs

As stated by the health authorities, CYPs are of high clinical relevance for DDIs. The CYPs constitute the major enzyme family capable of catalyzing oxidative biotransformation. Of the 57 putatively functional human CYPs, only about a dozen enzymes, belonging to the CYP 1, 2, and 3 families, are responsible for the biotransformation of most xenobiotics, including 70–80% of all drugs in clinical use [6]. CYPs 3A4, 2C9, 2C8, 2E1, and 1A2 are the highest expressed forms in the liver, while 2A6, 2D6, 2B6, 2C19, and 3A5 are less abundant, and CYPs 2 J2, 1A1, and 1B1 are mainly expressed extrahepatically [27]. The important CYP isoforms for DDIs are 1A2, 3A4/5, 2B6, 2C8, 2C9, 2C19, and 2D6 [4,28], and CYP3A4/5 is of the highest interaction ratio [2]. The high permeability drugs, mainly eliminated by metabolism, are often involved in CYPs-mediated DDIs.

Drug transporters are also crucial for DDIs. They are expressed in a variety of organs, including the intestine, liver, kidney, and brain, and they play a key role in the in vivo drug disposition, adverse reactions, and therapeutic efficacy of drugs [29]. The well-known transporters involved in DDIs are *P-gp*, BCRP, OATP1B1/OATP1B3, OAT1/OAT3, OCT2 and MATE1/MATE2K (Figure 1), and the poorly permeable drugs, predominantly eliminated by renal and/or biliary excretion, often suffer from transporter-mediated DDIs [30]. The hepatic uptake transporters are located on the basolateral membrane and mediate uptake or bidirectional transport of substrate drugs, and hepatic apical efflux transporters could take the drugs out of the hepatocytes into the blood or bile compartments. Inhibitions of hepatic uptake transporters, such as OATP1B1/3, play a significant role in transporter-mediated DDIs, mediating more than half of the severe DDIs with AUC changes > 5-fold [2,31]. Among the efflux transporters, interactions with *P-gp* are the most studied [32,33]. Due to the overlapping substrate specificity of *P-gp* and CYP3A, an inhibition of *P-gp* in the gut and liver can impact exposures of CYP3A substrates. Inhibition of *P-gp* may not result in clinically significant differences in the plasma exposure of the victim drug, but it can attenuate the efficacy of drugs targeting barrier tissues such as the brain, lymphocytes, and tumor [34].
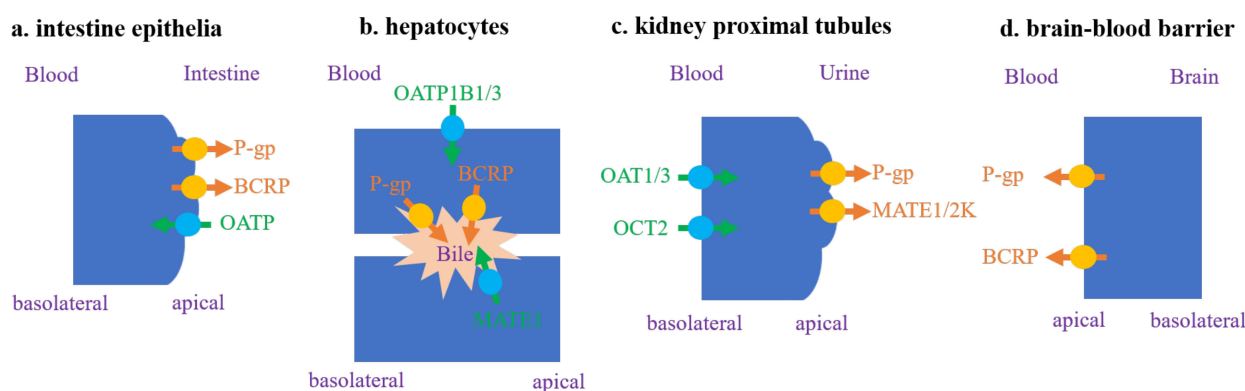
Figure 1. Transporters with a high clinical interest in drug–drug interactions (DDI) evaluation [4,28].

A candidate drug should be evaluated for its potential to be a perpetrator (inhibits or induces enzymes or transporters) or victim (whose PK is changed by a perpetrator) of DDIs with specific probe substrates, selective inhibitors or inducers, and second, with likely co-administered drugs. The alteration of drug-metabolizing enzyme activities can occur via three primary mechanisms: (1) reversible inhibition, (2) mechanism-based inactivation (MBI), and (3) induction [35]. The reversible mechanisms of inhibition can be competitive, noncompetitive and uncompetitive. Competitive inhibition, occurring in most cases, involves the inhibitor competing directly with the substrate for binding to the active site of the enzyme. In noncompetitive inhibition, the inhibitor binds at the allosteric site independently of substrate binding, meaning the inhibitor shares the same affinity for both enzyme and enzyme–substrate complex. This activity differentiates noncompetitive inhibition from uncompetitive inhibition, in which an inhibitor binds only to the enzyme–substrate complex [36]. MBI occurs when a compound undergoes a catalytic transformation by an enzyme to a species that, prior to release from the active site, inactivates the enzyme by either covalent or non-covalent binding. This indicates that the inhibitory effect may persist in vivo even after elimination of the inactivating species, and that the active enzyme can only be recovered by de novo synthesis. Induction occurs when a compound upregulates the synthesis of enzyme via receptor-mediated mechanisms (aryl hydrocarbon receptor (AhR) for CYP1A, constitutive androstane receptor (CAR) for CYP2B6, and pregnane X receptor (PXR) for CYP3A), affecting the transcription, translation and expression of that protein yielding a higher abundance within a given tissue mass [37].

Transporters-mediated DDIs follow the same inhibition or induction principles of CYPs-mediated DDIs [18,38]. The inhibition mechanism for most transporters is usually considered as only competitive, while OATP1B1/3 has been found to be inhibited by a few inhibitors via MBI [39–41]. The induction of transporters is most reported for *P-gp* [2].

3. In Vitro Tools for Determining Key PK DDIs Parameters

The evaluation of DDIs generally involves multiple processes, including mechanism clarification from preclinical/in vitro systems, model-based predictions, and final confirmation with clinical studies [42]. Due to the species difference in metabolizing enzymes and transporters between humans and animals, preclinical animal DDIs studies are not frequently adopted. Currently, the evaluation of DDIs usually begins with the in vitro experiments to determine the interaction mechanism and critical interaction parameters for the perpetrators and victims, and the derived parameters could be further implemented to the static and dynamic models.

3.1. Inhibition or Induction Potential of a Perpetrator

Preclinical prediction of CYPs inhibition mediated DDIs have been performed conventionally using the well-characterized and intensively studied human liver microsomes (HLM) and human hepatocytes (hHEPs) [42].

For reversible CYPs or transporter-mediated inhibition, the rate of turnover of the probe substrate is determined in the absence or presence of an inhibitor, using a matrix of varying substrate and inhibitor concentrations. Non-linear regression analysis is applied to the data to assess the type of inhibition and to obtain an estimate of the absolute inhibition constant (K_i). For a competitive enzyme inhibition, K_i is given by Equation (1) based on the Cheng–Prusoff equation [43], where IC_{50} is the inhibitor concentration required to inhibit 50% of the metabolic rate of a probe substrate, S is the substrate concentration, and k_m is the Michaelis–Menten constant for the substrate. Regarding the inhibition of transporters, the IC_{50} was often used as a practical substitute for the K_i, and the common in vitro systems for quantifying the inhibitory potency of transporter inhibitors are Caco-2 cells, HEK or MDCK transfected cells for uptake transporters, and membrane vesicles for efflux transporters [28].

$$K_i = \frac{IC_{50}}{1 + \frac{S}{K_m}}, \tag{1}$$

Estimation of the inactivation parameters of MBI integrates the steps of pre-incubation with different inhibitor concentrations for varying times, quenching with a dilution of the reaction mixture and further incubation after addition of the probe substrate in HLMs or hHEPs in plasma, followed by simultaneous fitting of the combined data set to obtain estimates of all in vitro kinetic parameters [1]. The pseudo-first-order rate constant (k_{obs}) is related to the maximum inactivation rate (k_{inact}) and the concentration required for half-maximal inactivation (K_I) as Equation (2) (equally applies to transporter involved MBI). The CYP natural degradation rate constant (k_{deg}) for the inactivated isoform is another key parameter for MBI. However, due to the challenges with methodology and sample size, there is a lack of consensus on turnover half-life ($t_{1/2}$) and a paucity of reported k_{deg} values for many of the CYPs involved in clinically relevant DDIs [44]. For hepatic CYP3A4, k_{deg} ranges from 0.0077 to 0.03 h^{-1} [45]. These values have been measured by three main in vitro approaches (1) measuring CYP apoprotein expression loss in liver models over time [46], (2) induction of CYP enzymes followed by tracking of de-induction recovery profiles [47], and (3) pulse-chase analysis after de-induction [48].

$$k_{obs} = \frac{k_{inact} \times I}{K_I + I}, \tag{2}$$

The most relevant in vitro models for studying drug induction are those using freshly cultured or cryopreserved hepatocytes [37]. The induction endpoint can be assessed via enzyme activities (most common), messenger RNA (mRNA) and CYPs protein content measurement (mechanistic). The magnitude of the induction effect can be described according to a calibration curve of relative induction scores (*RIS*), which is given by Equation (3). E_{max} is the maximum induction capacity, and EC_{50} is the effective concentration of the inducer at half-maximal induction. Due to the similarities of induction mechanism between CYPs and transporters, the induction equation for characterizing CYPs induction studies can also be applied to transporters induction studies, but currently, the in vitro systems to evaluate the induction of *P-gp* and other transporters are not well established [28].

$$RIS = \frac{E_{max} \times I_{max,\mu}}{EC_{50} + I_{max,\mu}}, \tag{3}$$

3.2. Reaction Phenotyping for Victim

For an accurate DDI prediction, it is important to quantitatively characterize relative contributions of the major enzyme(s) and/or transporter(s) involved in the clearance of victims, which is indicated by the parameters of fraction metabolized (f_m) and fraction transported (f_t). If an f_m or f_t value is greater than 0.25, the interaction between a victim drug and inhibitors/inducers of the relevant enzyme/transporter is considered significant [28].

The determination of f_m requires the identification of specific enzymes involved in a drug's metabolism. In vitro reaction phenotyping typically involves the incubation in HLMs or hHEPs with chemical inhibitors or antibodies and human recombinant P450 enzymes(rh-CYPs) [49,50]. By performing a series of incubations with various selective inhibitors for each of the main CYPs in HLMs or hHEPs, and comparing the relative metabolism rates (determined by measuring parent depletion or detecting metabolite formation), one can identify which inhibitor reduces the overall metabolism to the greatest extent and thereby uncover the metabolic pathway that contributes the most to the clearance of a compound. The percentage of inhibition observed will be the f_m for each enzyme [50,51]. To quantitatively translate the rh-CYPs data to f_m in HLMs or hHEPs, certain correlation factors are required, such as inter-system extrapolation factor (ISEF) or relative activity factor (RAF) [50].

Regarding the estimation of f_t, similar approaches based on RAF or relative expression factor (REF) have been proposed. For example, a hepatic clearance drug with a rate-determining process of the hepatic uptake across the basolateral membrane [52,53], the RAF and REF methods can be used to determine the f_t of the uptake transporters such as OATP1B1/3 [54,55]. The RAF method estimates the differences between the uptake rate in hHEPs (expresses multiple uptake transporters) and transfected cell lines with a specific transporter using relatively selective substrates, such as pitavastatin [54]. REF is usually obtained via Western blot analysis or LC–MS/MS-based protein quantification. Additionally, phenotyping approaches based on selective inhibitors or gene knockdown in primary hepatocytes can be employed to assess f_t [56,57]. The value of f_t is estimated by the uptake clearance in the absence (control) and presence of inhibitors, formulated as $f_t = 1 -$ (uptake clearance with each selective inhibitor/uptake clearance of control). These aforementioned strategies can also be applied for estimating the contribution of other transporters, such as the OATs/OCTs involved in renal tubular secretion.

4. Conventional Static Models for PK DDIs

4.1. Basic Model

PK DDIs is often evaluated by the overall change in the exposure of victim drug according to the ratio of the area under the plasma concentration-time profile of the victim drug in the presence and absence of a perpetrator (AUC^i/AUC), which can be calculated by Equation (4) based upon the hepatic "well-stirred" model [58]. Equation (4) assumes no transient plasma binding ($f_{\mu,b}$) displacement exists, the fraction absorbed (F_a) and the hepatic blood flow (Q_H) are not modified by the presence of a perpetrator, and the concentration of the perpetrator does not change over time. Furthermore, the metabolism of the victim drug is assumed to only occur in the liver, and metabolism is the only route of elimination. That is, the total clearance (CL) equals the hepatic clearance (CL_h). In this equation, F_h represents the hepatic drug availability, CL_h represents the hepatic clearance, $CL_{\mu,int}$ represents the unbound hepatic intrinsic clearance for a victim drug. $F_h{}^i$, $CL_h{}^i$, and $CL^i{}_{\mu,int}$ are the corresponding parameters in the presence of the perpetrator.

$$\frac{AUC^i_{p.o.}}{AUC_{p.o.}} = \frac{F_h^i}{F_h} \times \frac{CL_h}{CL_h^i} = \frac{\frac{Q_H}{Q_H+f_{\mu,b}\times CL^i_{\mu,int}}}{\frac{Q_H}{Q_H+f_{\mu,b}\times CL_{\mu,int}}} \times \frac{\frac{Q_H\times f_{\mu,b}\times CL_{\mu,int}}{Q_H+f_{\mu,b}\times CL_{\mu,int}}}{\frac{Q_H\times f_{\mu,b}\times CL^i_{\mu,int}}{Q_H+f_{\mu,b}\times CL^i_{\mu,int}}} = \frac{CL_{\mu,int}}{CL^i_{\mu,int}}, \tag{4}$$

The determination of $CL_{\mu,int}$ requires the in vitro enzyme kinetic studies, which are based upon the classical Michaelis–Menten equation (Equation (5)). v, V_{max}, K_m and S are the observed rate of metabolism (i.e., $CL_{\mu,int}$), the maximal velocity, the Michaelis–Menten constant, and the victim concentration, respectively. When the concentration of a substrate is much lower than its apparent K_m, the $CL_{\mu,int}$ equals to V_{max}/K_m [6].

$$v = \frac{V_{max} \times S}{K_m + S}, \tag{5}$$

In the presence of a perpetrator (inhibitor or inducer), the victim values of V_{max} and K_m will change. Accordingly, the ratio of $CL_{\mu,int}/CL^i_{\mu,int}$ can translate to the "R values", such as R_{rev-c}, R_{MBI}, and R_{ind}, which are, respectively representing the impact of competitive inhibition, MBI, and induction on $CL_{\mu,int}$. The standard calculation of these "R values" follows the Equations (6)–(8) according to the newest FDA DDI guideline [28]. In these equations, $I_{max,\mu}$ is the maximal unbound plasma concentration of perpetrator drug at steady state, $K_{i,\mu}$ is the unbound inhibition constant, and $K_{I,\mu}$ is the unbound inhibitor concentration causing half-maximal inactivation.

$$R_{rev-c} = 1 + \frac{I_{max,\mu}}{K_{i,\mu}},\tag{6}$$

$$R_{MBI} = 1 + \frac{k_{inact} \times I_{max,\mu}}{k_{deg} \times (K_{I,\mu} + I_{max,\mu})},\tag{7}$$

$$R_{ind} = 1 + \frac{E_{max} \times I_{max,\mu}}{EC_{50} + I_{max,\mu}},\tag{8}$$

Thus, the DDI potential (AUC^i/AUC) can be expressed directly by in vitro enzyme kinetic parameters after substituting Equations (6)–(8) into Equation (4). Taking competitive inhibition as an example, the extent of DDIs could be displayed by Equation (9), which represents the basic model of DDIs.

$$\frac{AUC^i_{p.o.}}{AUC_{p.o.}} = \frac{CL_{\mu,int}}{CL^i_{\mu,int}} = 1 + \frac{I_{max,\mu}}{K_{i,\mu}},\tag{9}$$

The basic models based on these "R values" are the most common methods adopted in DDI evaluation. For CYPs-mediated DDIs, if $R_{rev-c} \geq 1.02$, $R_{MBI} \geq 1.25$, or $R_{ind} \leq 0.8$ [59], the FDA suggests conducting further investigation of the DDI potential in mechanistic models or clinical DDI study with a sensitive probe substrate [28]. For transporter-mediated DDIs, the criteria differ [28]. If I_{gut}/IC_{50} or $K_i \geq 10$ (I_{gut} = dose of inhibitor/250 mL), the investigational drug (administered orally) has the potential to inhibit *P-gp* or BCRP in vivo. If $1 + ((f_{u,p} \times I_{in,max})/IC_{50}) \geq 1.1$, (where $I_{in,max}$ is the estimated maximum plasma inhibitor concentration at the inlet to the liver), the investigational drug has the potential to inhibit OATP1B1/3 in vivo. Moreover, if $I_{max,u}/IC_{50}$ value is ≥ 0.1, the investigational drug has the potential to inhibit OATs, OCTs, MATEs in vivo.

4.2. Mechanistic Static Model

The aforementioned equations are all based on the assumption that metabolism in the liver is the only route of the victim's elimination, which is obviously hard to match the real situation. Considering the oral administration, the metabolism often involves other organs (e.g., gut and kidney) with different enzymes or transporters located. To account for this discrepancy, the "Modified Rowland–Matin model" (Equation (10)) was proposed, where f^i means f_m or f_t as mentioned earlier [60–62]. The utility of this model is apparent when the victim is eliminated by several routes or involved multiple enzymes/transporters, as the percent contribution to the total clearance can be factored, and only the affected fraction (f^i) is inhibited.

$$\frac{AUC^i_{p.o.}}{AUC_{p.o.}} = \frac{CL_{\mu,int}}{CL^i_{\mu,int}} = \frac{1}{\frac{f^i}{1+\frac{I_\mu}{K_i}} + (1 - f^i)},\tag{10}$$

A limitation of the "Modified Rowland–Matin model" is the inability to distinguish the relative contributions of the enzyme- and transporter-mediated DDIs. For example, when an enzyme inhibitor is a substrate to a hepatic uptake transporter, the unbound intracellular concentration available at the target enzyme is different from the unbound plasma concentration [63], and the permeability of drug through membranes becomes

a rate-controlling process for hepatic clearance. In this case, the "Extended clearance concept" (Equation (11)) can clarify the primary role of transporters and incorporate the co-contribution of the enzymes and transporters to intrinsic hepatic clearance [56,64].

$$CL_{\mu,int,h} = (SF \times PS_{uptake} + PS_{dif,inf}) \times \frac{CL_{\mu,int,met} + PS_{efflux}}{PS_{dif,eff} + CL_{\mu,int,met} + PS_{efflux}}, \quad (11)$$

In this equation, PS_{uptake} represents the basolateral active uptake clearance, which can be obtained from in vitro uptake experiments utilizing hepatocyte or recombinant cell line systems, and $PS_{dif,inf}$ represents the basolateral passive diffusion. PS_{efflux} is intrinsic biliary clearance mediated by apical efflux transporters, derived from sandwich culture or vesicle experiments. $CL_{\mu,int,met}$ represents the total intrinsic metabolic clearance, and it is determined by conventional in vitro incubation systems (e.g., microsomes) [65–67]. SF represents the empirical scaling factor for matching the in vivo $CL_{\mu,int,h}$ [68].

By integrating the "extended clearance concept" with the specific transporter and enzyme inhibition/induction interactions, the most informative mechanistic static model— "net effect model" is obtained [69]. For instance, the competitive inhibition can be described by Equation (12) using this kind of mechanistic model.

$$CL^i_{\mu,int,h} = (\frac{SF \times PS_{uptake}}{R_{uptake}} + PS_{dif,inf}) \times \frac{\sum \frac{CL_{int,cyp}}{R_{cyp}} + \frac{PS_{efflux}}{R_{efflux}}}{PS_{dif,inf} + \sum \frac{CL_{int,cyp}}{R_{cyp}} + \frac{PS_{efflux}}{R_{efflux}}}, \quad (12)$$

where R_{uptake}, R_{cyp} and R_{efflux} represent the competitive inhibition terms for active hepatic uptake, particular CYP isoform and biliary efflux transport, respectively. This model has been validated for quantitative DDI predictions involving CYP enzymes and OATP1B by using a set of ten substrate drugs and five inhibitor drugs [66].

5. Dynamic PBPK Model for PK DDIs

5.1. Concept of PBPK Model

The PBPK model consists of a series of linked differential equations that are solved numerically on the computer to track the time course of drug concentrations in blood and tissues after dosing. A whole-body PBPK model is a mathematical representation of the body that integrates the physiology data, the organs that are most relevant to the absorption, distribution, excretion, and metabolization of the drug, and blood connections between the organs (Figure 2a). These organs are typically lung, brain, heart, gut, liver, kidney, adipose tissue, bone, and muscle, and each one of them is characterized by a combination of associated blood-flow rate, tissue volume, tissue-partition coefficient (K_p), and permeability [70,71]. Generally, PBPK models assume that each tissue compartment is well-stirred and perfusion rate limited, whereas permeability-limited distribution or disposition needs to be considered for large, hydrophilic molecules or transporter-dependent drugs (Figure 2b) [72].

The major PBPK applications (among PBPK-related publications) were associated with the study design, predicting formulation effects and metabolic DDIs, while studying the fate of drugs in special populations, predicting kinetics in early drug development, and investigating transporter-mediated DDIs have increased proportionally over the last decade [75]. In recent surveys of the PBPK-based submissions to FDA [76,77], about 56–67% of the submissions used PBPK modeling to evaluate the drug interaction potential.
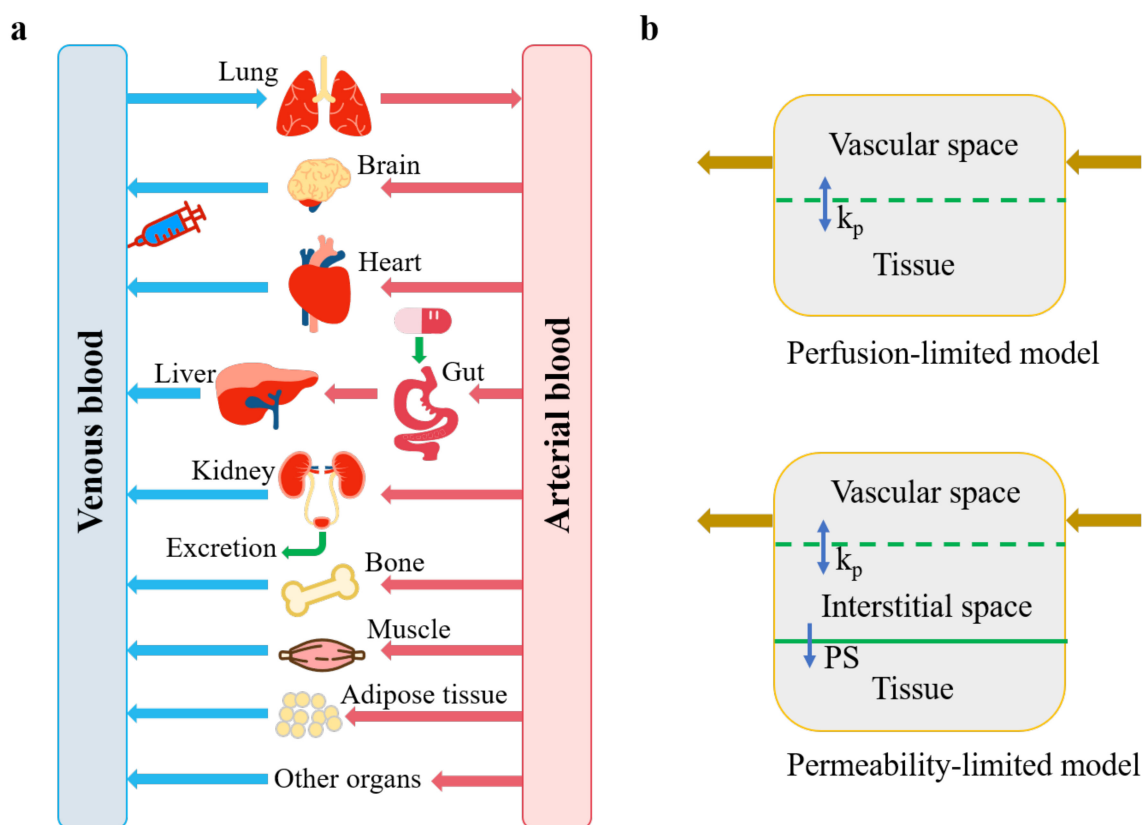
Figure 2. A generic physiologically based pharmacokinetic (PBPK) model (**a**) adapted from Shin, H.K. et al. [73], and 2 types of tissue model structure (**b**) adapted from Yuan, D. et al. [74]. k_p, tissue partitioning coefficient, namely concentration ratio between tissue and blood at steady state; *PS*, membrane permeability coefficient.

5.2. Strategy of PBPK Modeling to Solve PK DDIs

The PK DDIs between victim and perpetrator drugs in vivo is a dynamic process, and PBPK modeling is a perfect approach to characterize this time-varying interaction, thus enables more accurate predictions of DDIs than static models. Besides, PBPK models are embedded with the variance of extrinsic and intrinsic factors (e.g., CYPs or transporter abundance and activity). The simulation and prediction results in the virtual population can not only indicate the case of the average population but also account for the case of extreme individuals [78]. The use of PBPK modeling to evaluate DDI risk is usually carried out in a stepwise manner. First, separate PBPK models for the victim and perpetrator drugs should be developed and verified. Briefly, the physiochemistry information (e.g., *Log P* and pK_a) and in vitro metabolism/transporter data of the victim/perpetrator are plugged directly into a PBPK software tool, together with the integrated physiological parameters in the software, to obtain the preliminary parametrized initial model for the victim or perpetrator. The initial models are then verified/refined with clinical data (e.g., the PK profiles after intravenous or oral administration). Second, these two verified PBPK models (victim PBPK model and perpetrator PBPK model) are linked together by specific equations informed by the DDI mechanism derived from in vitro studies. Third, the DDI potential is predicted and verified with observed in vivo data (e.g., PK profiles, *AUC* and C_{max} ratios). The workflow for using PBPK modeling to predict CYPs/transporter-mediated DDIs are described in Figure 3 [38]. Notably, the victim PBPK model should integrate delicate system data (e.g., enzyme and transporter expression levels) and drug-related information (e.g., enzyme-level based metabolism and transport-based uptake/efflux rates) [79,80]. Also, it is necessary for the victim PBPK model to ensure both the plasma concentration versus time profile and the fraction of the systemic clearance via the enzyme/transporter in question are correctly captured [81]. For the perpetrator PBPK model, it is crucial to correctly predict

the unbound concentrations at the site of the drug interaction (e.g., intestine, liver, or kidneys) and provide accurate estimates of the interaction parameters (e.g., K_i, E_{max}). The above aspects are of key importance to simultaneously evaluate multiple inhibitions and induction mechanisms and to accurately predict the potential of DDIs [81,82].
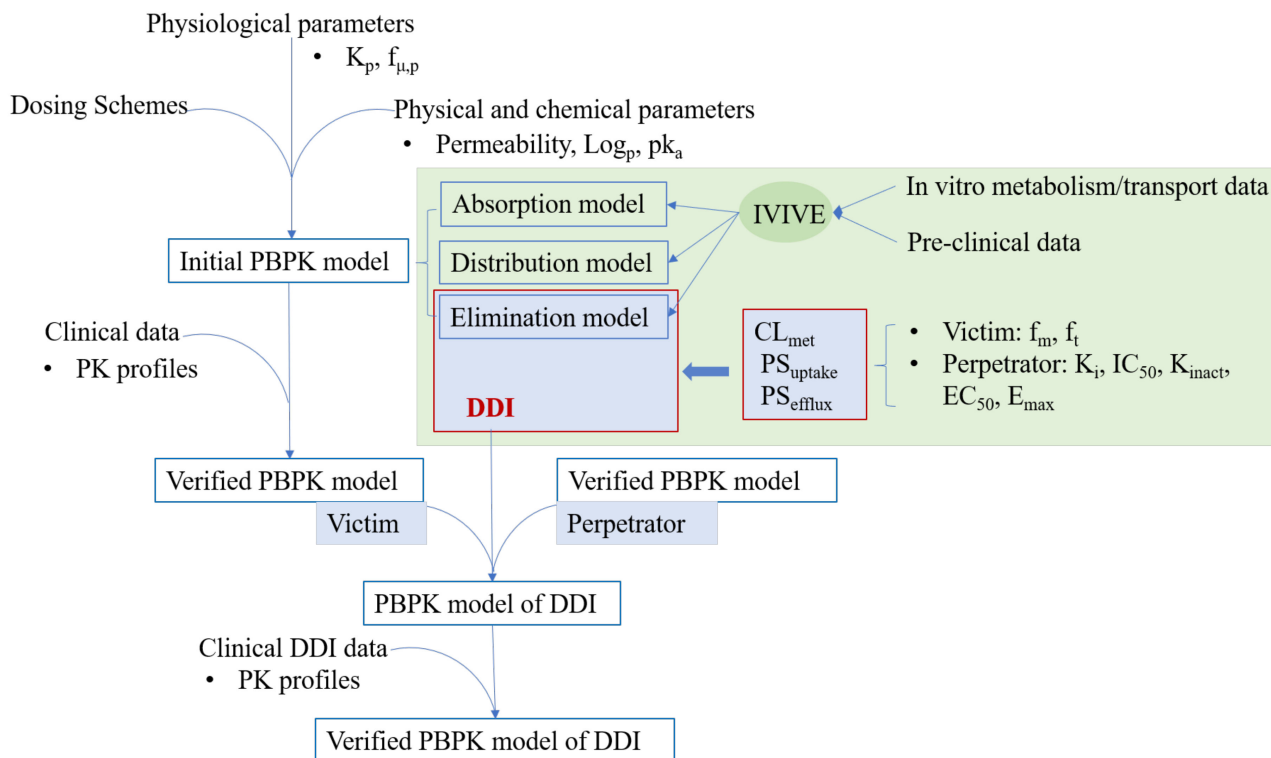

Figure 3. Workflow of PBPK modeling for the prediction of cytochromes P450 (CYP)/transporter-mediated DDIs.

The approaches to building a PBPK model have been well discussed in detail by Shebley et al. [81]. Usually, the bottom-up approach is the preferred option because it provides the mechanistic understanding of the drug's metabolism and excretion based on in vitro data of the CYPs and transporters of interest. When the in vitro data are not available, the retrograde model based on the top-down or middle-out approaches can be applied. The frequently used PBPK software tools that possess capabilities for DDIs modeling are PK-Sim [83], Simcyp [84], and GastroPlus™ [85].

5.3. Key Differential Equations for DDIs in PBPK Modeling

Depending on the critical elimination pathways of a victim drug, the CYPs and transporters may coordinately contribute to the drug's disposition. The CYPs mainly participate in hepatic and intestinal metabolism, the *P-gp* and BCRP transporters usually involve in the PK DDIs in the processes of intestinal absorption, bile secretion (canaliculus efflux) and renal secretion and the OATP transporters may dominate the hepatic clearance [20,25,86]. A clinically relevant DDI may occur when the perpetrator affects one of the main pathways of the victim drug. To give an in-depth understanding of how various interactions between victim and perpetrator are handled by the PBPK modeling approach, here we summarized the key differential equations for different DDI mechanisms. Considering the in vivo main pathways of a drug, the key differential equations for the DDIs within a simplified PBPK model concentrate on three modules—Portal vein (where the drug firstly comes into the systemic circulation from the gut), Liver (where the drug is metabolized or biliary excreted) and Systemic compartment (containing blood vessels, kidneys, and other non-eliminating organs). The simplified structure for these three modules is shown in Figure 4 [20,87]. Renal drug clearance (CL_R) is defined by the sum of glomerular filtra-

tion (CL_{fil}) and tubular secretion (CL_{sec}) minus tubular reabsorption (CL_{reabs}). Most renal DDIs are linked to inhibition of drug transporters (OATs, OCTs) for tubular secretion. The static or dynamic models to evaluate the transporter-mediated DDIs in the kidney follow the same principles as the transporter-mediated DDIs in the liver/intestine [88,89]. For simplicity, the transporter-mediated DDI in renal elimination is not presented below.
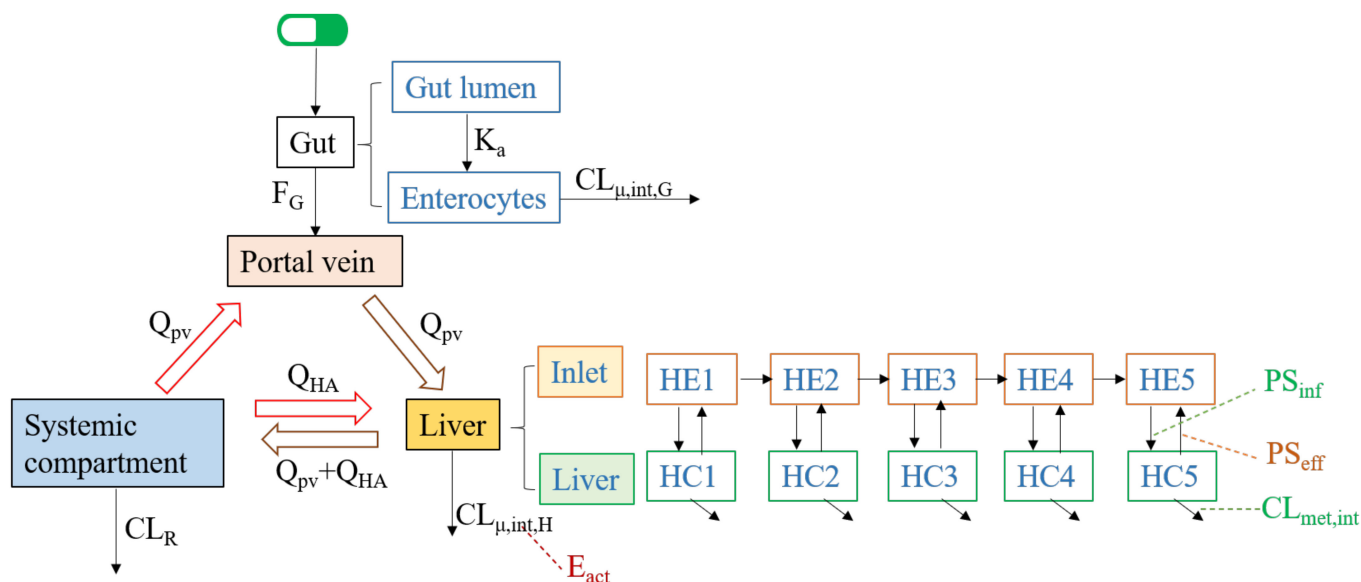

Figure 4. Sketch for major compartmental modules and related parameters. The subscripts of *pv, G, H, HA* and *sys* represent the portal vein, gut, liver, hepatic artery and systemic compartment, respectively. *Q* is the blood flow rate, K_a is the absorption rate constant, F_G is gut availability after intestinal metabolism; $CL_{\mu,int,H}$ and $CL_{\mu,int,H}$ are the unbound intrinsic clearance in liver and enterocytes. PS_{inf} is the overall influx intrinsic clearance, PS_{eff} is the overall efflux intrinsic clearance, and $CL_{met,int}$ represents the hepatic metabolism by CYPs.

When the intestinal or hepatic metabolism is the major elimination pathway and the drug entering the liver is a perfusion-limited process, the concentrations of the victim drug in the portal vein, liver, and systemic compartment can be described by Equations (13)–(15) [87].

$$\frac{dC_{pv}}{dt} \times V_{pv} = (C_{sys} - C_{pv}) \times Q_{pv} + f_a \times \frac{Q_G}{Q_G + f_{\mu,G} \times CL_{\mu,int,G}(t)} \times k_a \times D \times e^{-k_a \times t}, \tag{13}$$

$$\frac{dC_{liver}}{dt} \times V_{liver} = Q_{pv} \times C_{pv} + Q_{HA} \times C_{sys} - [f_{\mu,B} \times CL_{\mu,int,H}(t) + Q_{pv} + Q_{HA}] \times C_{liver}, \tag{14}$$

$$\frac{dC_{sys}}{dt} \times V_{sys} = (Q_{pv} + Q_{HA}) \times C_{liver} - (\frac{CL_R}{f_{\mu,B}} + Q_{pv} + Q_{HA}) \times C_{sys}, \tag{15}$$

where *C* is the unbound drug concentration, *V* is the compartmental volume, f_a means the fraction of dose absorbed from the gut lumen, $f_{\mu,G}$ and $f_{\mu,B}$ represents the unbound drug fraction in gut and blood, and *D* is the total drug amount.

If the hepatic uptake transporters such as OATP1B1/3 and OATP2B1 dominate the drug elimination, the drug entering the liver becomes a permeability-limited process. In this case, the liver can be subdivided into the extrahepatic (inlet) and hepatocellular (liver) compartments, which were divided into five small compartments sequentially connected by hepatic blood flow to mimic the dispersion model [90]. The mass balance differential equations for these two compartments could be described by Equations (16) and (17) [20]:

$$\frac{dC_{inlet}}{dt} \times V_{inlet} = Q_h(C_{sys} - C_{inlet}) - f_{\mu,B} \times PS_{inf} \times C_{inlet} + f_{\mu,H} \times PS_{eff} \times C_{liver}, \tag{16}$$

$$\frac{dC_{liver}}{dt} \times V_{liver} = f_{\mu,B} \times PS_{inf} \times C_{inlet} - f_{\mu,H} \times (PS_{eff} + CL_{met,int}) \times C_{liver}, \tag{17}$$

where Q_h is the hepatic blood flow rate, PS_{inf} consists of the active uptake intrinsic clearance on the basolateral membrane by uptake transporters (PS_{uptake}) and the influx intrinsic clearance by passive diffusion on the basolateral membrane ($PS_{dif,inf}$), and PS_{eff} consists of the intrinsic efflux clearance of canaliculus efflux transporters (PS_{efflux}) and the intrinsic efflux clearance by passive diffusion on the basolateral membrane ($PS_{dif,eff}$).

A perpetrator drug affects the victim drug by increasing or decreasing the victim's $CL_{\mu,int}$, PS_{uptake} or PS_{efflux}. For enzyme-based metabolism, Equation (18) shows the $CL_{\mu,int}$ of the victim drug in the absence of the perpetrator, and Equation (19) indicates the dynamic changes of the $CL_{\mu,int}$ of the victim drug in the presence of the perpetrator. Regarding the transporter-mediated elimination, the impact of the perpetrator on the PS_{uptake} and/or PS_{efflux} of the victim drug can be determined in a similar way as $CL_{\mu,int}$ [82]. If intestine clearance can be ignored and $CL_{\mu,int,h}$ in the liver is known, $CL_{\mu,int}$, PS_{uptake}, and PS_{efflux} can be obtained from Equation (11) ("extended clearance concept") via back-calculation.

$$CL_{\mu,int} = \frac{V_{max} \times SF}{K_m + f_{\mu,B} \times C_{liver/gut}}, \tag{18}$$

$$CL_{\mu,int}(t) = \frac{CL_{\mu,int}}{R_{rev-c}} \times \left[1 + f^i{}_{cyp} \times \left(\frac{E_{act}(t)}{E_0} - 1\right)\right], \tag{19}$$

where $f^i{}_{cyp}$ is the fractional CYP-mediated metabolism to $CL_{\mu,int}$, $E_{act,H}$ is the active amounts of the enzyme in the liver, and E_0 represents the enzyme amounts at baseline. R_{rev-c} indicates the competitive inhibition.

As $CL_{\mu,int}$ is related to the amount and activity of the metabolizing enzyme (E_{act}), the $CL_{\mu,int}$ would change along with the E_{act} if the perpetrator inactivates or induces the metabolizing enzyme. This time-varying amount of the active enzyme can be described by Equation (20). R_{ind} and R_{MBI} indicate the induction and MBI by the perpetrator.

$$\frac{dE_{act,H}}{dt} = -k_{deg} \times E_0 \times R_{ind} - E_{act,H} \times R_{MBI}, \tag{20}$$

To sum up, a PBPK model of DDI is a mathematical model constructed by the above key equations. The Equations (13)–(17) are differential expression indicating the flow of drug along with blood in the body, and the Equations (18)–(20) account for the drug interaction through a dynamic change of CL_{int} and E_{act}.

6. Current Status and Future Perspectives

The static model assumes that the concentration of a perpetrator is at the maximum concentration and tends to overpredict DDI risk. Different from the static model, the PBPK approach considers the temporal changes in inhibitor and substrate concentrations, the complex dosing regimens of the inhibitor and substrate, and the time-dependent changes in enzyme abundance, which is especially important for MBI and induction. Therefore, the PBPK model allows a full characterization of the in vivo concentration-time course and a more accurate determination of the magnitude of DDIs. In addition, the PBPK modeling allows high confidence in prospective DDI predictions considering the interindividual variability in enzyme expression levels arising from genetic, anatomical, demographic, and pathophysiological differences. Overall, PBPK models are useful tools to aid the design and interpretation of clinical drug-interaction studies and are of great value for assessing and delineating DDIs potential in patient populations.

Yet, as an advanced approach, the PBPK modeling relies on the quality of in vitro data and the accuracy of IVIVE [79]. Moreover, compared to CYP enzymes, the experience of using the PBPK model for transporter-based DDIs is limited, and the corresponding predictive performance is not that well. This is largely due to knowledge gaps in transporter biology and limited experience in determining and modeling the kinetics of transporters. The poor IVIVE for transport-related clearance and DDI prediction may be addressed by ensuring that each in vitro system responds appropriately to test substrates and inhibitors.

One direction in this field is to screen the specific endogenous biomarkers for drug transporters, and this may aid the DDI risk assessment. There have been some potentially useful biomarkers reported for transporter functions, and they were recently reviewed [91]. For instance, the biomarkers for OATP1B hepatic uptake transporter includes coproporphyrins I and III (CP-I/III), tetradecanedioate, and glycochenodeoxycholate sulfate, and the biomarker N1-methylnicotinamide is targeted for MATE-mediated renal secretion. On the other hand, the gap of accurate DDIs prediction in tissues is also needed to be filled. The use of positron emission tomography (PET) imaging technology may be a doable way to identify the rate-determining process in tissues by detecting the tissue time-course of the radiolabeled transporter substrates [92,93]. In the future, PBPK modeling of the transporters is expected to approach the state of maturity, like currently the case of CYPs, by using the well-established screening assays to generate reliable data used for IVIVE.

Another important question to answer is when to use the static or the dynamic model for the DDI evaluation. The US FDA has made a good recommendation based on the typical basic model, modified Rowland–Martin model and PBPK model. First, one can start with the basic model and compare the calculated "R values" to predefined cutoff criteria to determine whether it is possible to rule out the potential for a DDI [28]. Second, if the basic model does not rule out the potential for DDIs, additional modeling analyses, using modified Rowland–Martin model or PBPK models to proactively understand the DDI risk and avoid unnecessary DDI trials are suggested. Last, if the predicted AUC^i/AUC of a sensitive index substrate in the presence and absence of an investigational drug is ≤0.8 (induction) or ≥1.25 (inhibition) based on mechanistic models, and in vivo DDIs study is suggested to verify/negate the model predictions [77].

In recent years, we have witnessed an acceleration of the growing-up of PBPK [94]. With the mature of in vitro technologies and the buildup of PBPK system knowledge (enzyme/transporter abundance, physiological parameters, the effect of disease, age, sex, and polymorphism status), the empirical static approaches may be phased out. To promote the use of PBPK modeling, investment in education is needed to train more specialists in modeling and simulation. In addition, knowledge-sharing should be advocated in this field. This can be done by submitting the PBPK substance models, system parameters, and DDIs cases to open and publicly available platforms/ repositories.

7. Conclusions

This review has elucidated the mechanisms, the in vitro methods, and the static or dynamic models for CYPs/transporter-mediated PK DDIs. A perpetrator drug could inhibit or induce the CYPs/transporters responsible for the elimination of the victim drug, resulting in an increase or decrease of the victim's exposure in vivo. To evaluate the DDIs mechanism and magnitude, HLMs, hHEPs and recombinant cell systems could be employed to determine the perpetrator's intensity of influence to the victim and the victim's susceptibility to interaction. The classic static models such as the basic model, the modified Rowland–Matin model, and the net effect model could be used as startup approaches to assess the potential risk of DDIs. As a dynamic and most informative in silico DDI evaluation tool, the PBPK model is increasingly advocated for DDIs predictions, particularly in cases where static models are inadequate to capture the overall DDI liability. Currently, there is still a big challenge to fill the data availability gap of transporters to improve the quality of DDI predictions, while the ongoing work and efforts could definitely shape the future.

Author Contributions: Y.P. Conceptualization, F.X.; literature search, Y.P.; writing—original draft preparation, Y.P.; writing—review and editing, F.X. and Z.C.; All authors have read and agreed to the published version of the manuscript.

Conflicts of Interest: The authors declare no conflict of interest.

References

1. Lu, C.; Di, L. In vitro and in vivo methods to assess pharmacokinetic drug- drug interactions in drug discovery and development. *Biopharm. Drug Dispos.* **2020**, *41*, 3–31. [CrossRef] [PubMed]
2. Yu, J.; Petrie, I.D.; Levy, R.H.; Ragueneau-Majlessi, I. Mechanisms and Clinical Significance of Pharmacokinetic-Based Drug-Drug Interactions with Drugs Approved by the U.S. Food and Drug Administration in 2017. *Drug Metab. Dispos.* **2019**, *47*, 135–144. [CrossRef] [PubMed]
3. Baneyx, G.; Fukushima, Y.; Parrott, N. Use of physiologically based pharmacokinetic modeling for assessment of drug–drug interactions. *Future Med. Chem.* **2012**, *4*, 681–693. [CrossRef]
4. Guideline on the Investigation of Drug Interactions. Available online: https://www.ema.europa.eu/en/documents/scientific-guideline/guideline-investigation-drug-interactions-revision-1_en.pdf (accessed on 3 December 2020).
5. Clinical Drug Interaction Studies—Cytochrome P450 Enzymes- and Transporter-Mediated Drug Interactions Guidance for Industry. Available online: https://www.fda.gov/regulatory-information/search-fda-guidance-documents/clinical-drug-interaction-studies-cytochrome-p450-enzyme-and-transporter-mediated-drug-interactions (accessed on 3 December 2020).
6. Wienkers, L.C.; Heath, T.G. Predicting in vivo drug interactions from in vitro drug discovery data. *Nat. Rev. Drug Discov.* **2005**, *4*, 825–833. [CrossRef]
7. Giacomini, K.M.; Krauss, R.M.; Roden, D.M.; Eichelbaum, M.; Hayden, M.R.; Nakamura, Y. When good drugs go bad. *Nature* **2007**, *446*, 975–977. [CrossRef] [PubMed]
8. Honig, P.K.; Woosley, R.L.; Zamani, K.; Conner, D.P.; Cantilena, L.R., Jr. Changes in the pharmacokinetics and electrocardiographic pharmacodynamics of terfenadine with concomitant administration of erythromycin. *Clin. Pharmacol. Ther.* **1992**, *52*, 231–238. [CrossRef] [PubMed]
9. Boulenc, X.; Barberan, O. Metabolic-based drug-drug interactions prediction, recent approaches for risk assessment along drug development. *Drug Metab. Drug Interact.* **2011**, *26*, 147–168. [CrossRef] [PubMed]
10. Pan, Y.; Hsu, V.; Grimstein, M.; Zhang, L.; Arya, V.; Sinha, V.; Grillo, J.A.; Zhao, P. The Application of Physiologically Based Pharmacokinetic Modeling to Predict the Role of Drug Transporters: Scientific and Regulatory Perspectives. *J. Clin. Pharmacol.* **2016**, *56*, 122–131. [CrossRef]
11. Zhang, X.; Quinney, S.K.; Gorski, J.C.; Jones, D.R.; Hall, S.D. Semiphysiologically based pharmacokinetic models for the inhibition of midazolam clearance by diltiazem and its major metabolite. *Drug Metab. Dispos.* **2009**, *37*, 1587–1597. [CrossRef]
12. Bois, F.Y. Physiologically based modelling and prediction of drug interactions. *Basic Clin. Pharmacol. Toxicol.* **2010**, *106*, 154–161. [CrossRef]
13. Fenneteau, F.; Poulin, P.; Nekka, F. Physiologically based predictions of the impact of inhibition of intestinal and hepatic metabolism on human pharmacokinetics of CYP3A substrates. *J. Pharm. Sci.* **2010**, *99*, 486–514. [CrossRef] [PubMed]
14. Manikandan, P.; Nagini, S. Cytochrome P450 Structure, Function and Clinical Significance: A Review. *Curr. Drug Targets* **2018**, *19*, 38–54. [CrossRef] [PubMed]
15. Riley, R.J.; Wilson, C.E. Cytochrome P450 time-dependent inhibition and induction: Advances in assays, risk analysis and modelling. *Expert Opin. Drug Metab. Toxicol.* **2015**, *11*, 557–572. [CrossRef] [PubMed]
16. Fowler, S.; Morcos, P.N.; Cleary, Y.; Martin-Facklam, M.; Parrott, N.; Gertz, M.; Yu, L. Progress in Prediction and Interpretation of Clinically Relevant Metabolic Drug-Drug Interactions: A Minireview Illustrating Recent Developments and Current Opportunities. *Curr. Pharmacol. Rep.* **2017**, *3*, 36–49. [CrossRef]
17. Dmitriev, A.V.; Lagunin, A.A.; Karasev, D.A.; Rudik, A.V.; Pogodin, P.V.; Filimonov, D.A.; Poroikov, V.V. Prediction of Drug-Drug Interactions Related to Inhibition or Induction of Drug-Metabolizing Enzymes. *Curr. Top. Med. Chem.* **2019**, *19*, 319–336. [CrossRef]
18. Varma, M.V.; El-Kattan, A.F. Transporter-Enzyme Interplay: Deconvoluting Effects of Hepatic Transporters and Enzymes on Drug Disposition Using Static and Dynamic Mechanistic Models. *J. Clin. Pharmacol.* **2016**, *56*, 99–109. [CrossRef]
19. Cerny, M.A. Prevalence of Non-Cytochrome P450-Mediated Metabolism in Food and Drug Administration-Approved Oral and Intravenous Drugs: 2006–2015. *Drug Metab. Dispos.* **2016**, *44*, 1246–1252. [CrossRef]
20. Watanabe, T.; Kusuhara, H.; Maeda, K.; Shitara, Y.; Sugiyama, Y. Physiologically based pharmacokinetic modeling to predict transporter-mediated clearance and distribution of pravastatin in humans. *J. Pharmacol. Exp. Ther.* **2009**, *328*, 652–662. [CrossRef]
21. Barton, H.A.; Lai, Y.; Goosen, T.C.; Jones, H.M.; El-Kattan, A.F.; Gosset, J.R.; Lin, J.; Varma, M.V. Model-based approaches to predict drug-drug interactions associated with hepatic uptake transporters: Preclinical, clinical and beyond. *Expert Opin. Drug Metab. Toxicol.* **2013**, *9*, 459–472. [CrossRef]
22. Wang, Q.; Zheng, M.; Leil, T. Investigating Transporter-Mediated Drug-Drug Interactions Using a Physiologically Based Pharmacokinetic Model of Rosuvastatin. *CPT Pharmacomet. Syst. Pharmacol.* **2017**, *6*, 228–238. [CrossRef]
23. Otsuka, Y.; Choules, M.P.; Bonate, P.L.; Komatsu, K. Physiologically-based Pharmacokinetic Modeling for the Prediction of a Drug-Drug Interaction of Combined Effects on P-gp and CYP3A. *CPT Pharmacomet. Syst. Pharmacol.* **2020**, *9*, 659–669. [CrossRef] [PubMed]
24. Elmeliegy, M.; Vourvahis, M.; Guo, C.; Wang, D.D. Effect of P-glycoprotein (P-gp) Inducers on Exposure of P-gp Substrates: Review of Clinical Drug-Drug Interaction Studies. *Clin. Pharmacokinet.* **2020**, *59*, 699–714. [CrossRef] [PubMed]

25. Bae, S.H.; Park, W.S.; Han, S.; Park, G.J.; Lee, J.; Hong, T.; Jeon, S.; Yim, D.S. Physiologically-based pharmacokinetic predictions of intestinal BCRP-mediated drug interactions of rosuvastatin in Koreans. *Korean J. Physiol. Pharmacol.* **2018**, *22*, 321–329. [CrossRef]

26. Varma, M.V.; Pang, K.S.; Isoherranen, N.; Zhao, P. Dealing with the complex drug-drug interactions: Towards mechanistic models. *Biopharm. Drug Dispos.* **2015**, *36*, 71–92. [CrossRef] [PubMed]

27. Zanger, U.M.; Schwab, M. Cytochrome P450 enzymes in drug metabolism: Regulation of gene expression, enzyme activities, and impact of genetic variation. *Pharmacol. Ther.* **2013**, *138*, 103–141. [CrossRef]

28. In Vitro Drug Interaction Studies—Cytochrome P450 Enzymes- and Transporter-Mediated Drug Interactions Guidance for Industry. Available online: https://www.fda.gov/regulatory-information/search-fda-guidance-documents/vitro-drug-interaction-studies-cytochrome-p450-enzyme-and-transporter-mediated-drug-interactions (accessed on 3 December 2020).

29. Giacomini, K.M.; Huang, S.M.; Tweedie, D.J.; Benet, L.Z.; Brouwer, K.L.; Chu, X.; Dahlin, A.; Evers, R.; Fischer, V.; Hillgren, K.M.; et al. Membrane transporters in drug development. *Nat. Rev. Drug Discov.* **2010**, *9*, 215–236.

30. Varma, M.V.; Gardner, I.; Steyn, S.J.; Nkansah, P.; Rotter, C.J.; Whitney-Pickett, C.; Zhang, H.; Di, L.; Cram, M.; Fennerm, K.S.; et al. pH-Dependent solubility and permeability criteria for provisional biopharmaceutics classification (BCS and BDDCS) in early drug discovery. *Mol. Pharm.* **2012**, *9*, 1199–1212. [CrossRef]

31. Yu, J.; Zhou, Z.; Tay-Sontheimer, J.; Levy, R.H.; Ragueneau-Majlessi, I. Risk of Clinically Relevant Pharmacokinetic-Based Drug-Drug Interactions with Drugs Approved by the U.S. Food and Drug Administration Between 2013 and 2016. *Drug Metab. Dispos.* **2018**, *46*, 835–845. [CrossRef]

32. Tachibana, T.; Kato, M.; Takano, J.; Sugiyama, Y. Predicting drug-drug interactions involving the inhibition of intestinal CYP3A4 and P-glycoprotein. *Curr. Drug Metab.* **2010**, *11*, 762–777. [CrossRef]

33. Fenner, K.S.; Troutman, M.D.; Kempshall, S.; Cook, J.A.; Ware, J.A.; Smith, D.A.; Lee, C.A. Drug-drug interactions mediated through P-glycoprotein: Clinical relevance and in vitro-in vivo correlation using digoxin as a probe drug. *Clin. Pharmacol. Ther.* **2009**, *85*, 173–181. [CrossRef]

34. Lee, C.A.; Cook, J.A.; Reyner, E.L.; Smith, D.A. P-glycoprotein related drug interactions: Clinical importance and a consideration of disease states. *Expert Opin. Drug Metab. Toxicol.* **2010**, *6*, 603–619. [CrossRef] [PubMed]

35. Obach, R.S.; Walsky, R.L.; Venkatakrishnan, K. Mechanism-based inactivation of human cytochrome p450 enzymes and the prediction of drug-drug interactions. *Drug Metab. Dispos.* **2007**, *35*, 246–255. [CrossRef] [PubMed]

36. Delaune, K.P.; Alsayouri, K. *Physiology, Noncompetitive Inhibitor, in StatPearls*; StatPearls Publishing: Treasure Island, FL, USA, 2020.

37. Hewitt, N.J.; Lechon, M.J.; Houston, J.B.; Hallifax, D.; Brown, H.S.; Maurel, P.; Kenna, J.G.; Gustavsson, L.; Lohmann, C.; Skonberg, C.; et al. Primary hepatocytes: Current understanding of the regulation of metabolic enzymes and transporter proteins, and pharmaceutical practice for the use of hepatocytes in metabolism, enzyme induction, transporter, clearance, and hepatotoxicity studies. *Drug Metab. Rev.* **2007**, *39*, 159–234. [CrossRef] [PubMed]

38. Taskar, K.S.; Pilla Reddy, V.; Burt, H.; Posada, M.M.; Varma, M.; Zheng, M.; Ullah, M.; Emami Riedmaier, A.; Umehara, K.I.; Snoeys, J.; et al. Physiologically-Based Pharmacokinetic Models for Evaluating Membrane Transporter Mediated Drug-Drug Interactions: Current Capabilities, Case Studies, Future Opportunities, and Recommendations. *Clin. Pharmacol. Ther.* **2020**, *107*, 1082–1115. [CrossRef] [PubMed]

39. Gertz, M.; Cartwright, C.M.; Hobbs, M.J.; Kenworthy, K.E.; Rowland, M.; Houston, J.B.; Galetin, A. Cyclosporine inhibition of hepatic and intestinal CYP3A4, uptake and efflux transporters: Application of PBPK modeling in the assessment of drug-drug interaction potential. *Pharm. Res.* **2013**, *30*, 761–780. [CrossRef] [PubMed]

40. Izumi, S.; Nozaki, Y.; Maeda, K.; Komori, T.; Takenaka, O.; Kusuhara, H.; Sugiyama, Y. Investigation of the impact of substrate selection on in vitro organic anion transporting polypeptide 1B1 inhibition profiles for the prediction of drug-drug interactions. *Drug Metab. Dispos.* **2015**, *43*, 235–247. [CrossRef]

41. Pahwa, S.; Alam, K.; Crowe, A.; Farasyn, T.; Neuhoff, S.; Hatley, O.; Ding, K.; Yue, W. Pretreatment With Rifampicin and Tyrosine Kinase Inhibitor Dasatinib Potentiates the Inhibitory Effects Toward OATP1B1- and OATP1B3-Mediated Transport. *J. Pharm. Sci.* **2017**, *106*, 2123–2135. [CrossRef]

42. Yoshida, K.; Zhao, P.; Zhang, L.; Abernethy, D.R.; Rekic, D.; Reynolds, K.S.; Galetin, A.; Huang, S.M. In Vitro-In Vivo Extrapolation of Metabolism- and Transporter-Mediated Drug-Drug Interactions-Overview of Basic Prediction Methods. *J. Pharm. Sci.* **2017**, *106*, 2209–2213. [CrossRef]

43. Cheng, Y.; Prusoff, W. Relationship between the inhibition constant (K1) and the concentration of inhibitor which causes 50 percent inhibition (I50) of an enzymatic reaction. *Biochem. Pharmacol.* **1973**, *22*, 3099–3108.

44. Chan, C.Y.S.; Roberts, O.; Rajoli, R.K.R.; Liptrott, N.J.; Siccardi, M.; Almond, L.; Owen, A. Derivation of CYP3A4 and CYP2B6 degradation rate constants in primary human hepatocytes: A siRNA-silencing-based approach. *Drug Metab. Pharmacokinet.* **2018**, *33*, 179–187. [CrossRef]

45. Friedman, E.J.; Fraser, I.P.; Wang, Y.H.; Bergman, A.J.; Li, C.C.; Larson, P.J.; Chodakewitz, J.; Wagner, J.A.; Stoch, S.A. Effect of different durations and formulations of diltiazem on the single-dose pharmacokinetics of midazolam: How long do we go? *J. Clin. Pharmacol.* **2011**, *51*, 1561–1570. [CrossRef]

46. Renwick, A.B.; Watts, P.S.; Edwards, R.J.; Barton, P.T.; Guyonnet, I.; Price, R.J.; Tredger, J.M.; Pelkonen, O.; Boobis, A.R.; Lake, B.G.; et al. Differential maintenance of cytochrome P450 enzymes in cultured precision-cut human liver slices. *Drug Metab. Dispos.* **2000**, *28*, 1202–1209. [PubMed]

47. Ramsden, D.; Zhou, J.; Tweedie, D.J. Determination of a Degradation Constant for CYP3A4 by Direct Suppression of mRNA in a Novel Human Hepatocyte Model, HepatoPac. *Drug Metab. Dispos.* **2015**, *43*, 1307–1315. [CrossRef] [PubMed]
48. Takahashi, R.H.; Shahidi-Latham, S.K.; Wong, S.; Chang, J.H. Applying Stable Isotope Labeled Amino Acids in Micropatterned Hepatocyte Coculture to Directly Determine the Degradation Rate Constant for CYP3A4. *Drug Metab. Dispos.* **2017**, *45*, 581–585. [CrossRef] [PubMed]
49. Zientek, M.A.; Youdim, K. Reaction phenotyping: Advances in the experimental strategies used to characterize the contribution of drug-metabolizing enzymes. *Drug Metab. Dispos.* **2015**, *43*, 163–181. [CrossRef]
50. Di, L. Reaction phenotyping to assess victim drug-drug interaction risks. *Expert Opin. Drug Discov.* **2017**, *12*, 1105–1115. [CrossRef]
51. Zhang, H.; Davis, C.D.; Sinz, M.W.; Rodrigues, A.D. Cytochrome P450 reaction-phenotyping: An industrial perspective. *Expert Opin. Drug Metab. Toxicol.* **2007**, *3*, 667–687. [CrossRef]
52. Varma, M.V.; Steyn, S.J.; Allerton, C.; El-Kattan, A.F. Predicting Clearance Mechanism in Drug Discovery: Extended Clearance Classification System (ECCS). *Pharm. Res.* **2015**, *32*, 3785–3802. [CrossRef]
53. Shitara, Y.; Maeda, K.; Ikejiri, K.; Yoshida, K.; Horie, T.; Sugiyama, Y. Clinical significance of organic anion transporting polypeptides (OATPs) in drug disposition: Their roles in hepatic clearance and intestinal absorption. *Biopharm. Drug Dispos.* **2013**, *34*, 45–78. [CrossRef]
54. Mitra, P.; Weinheimer, S.; Michalewicz, M.; Taub, M.E. Prediction and Quantification of Hepatic Transporter-Mediated Uptake of Pitavastatin Utilizing a Combination of the Relative Activity Factor Approach and Mechanistic Modeling. *Drug Metab. Dispos.* **2018**, *46*, 953–963. [CrossRef]
55. Kunze, A.; Huwyler, J.; Camenisch, G.; Poller, B. Prediction of organic anion-transporting polypeptide 1B1- and 1B3-mediated hepatic uptake of statins based on transporter protein expression and activity data. *Drug Metab. Dispos.* **2014**, *42*, 1514–1521. [CrossRef] [PubMed]
56. Kimoto, E.; Obach, R.S.; Varma, M.V.S. Identification and quantitation of enzyme and transporter contributions to hepatic clearance for the assessment of potential drug-drug interactions. *Drug Metab. Pharmacokinet.* **2020**, *35*, 18–29. [CrossRef] [PubMed]
57. Bi, Y.A.; Costales, C.; Mathialagan, S.; West, M.; Eatemadpour, S.; Lazzaro, S.; Tylaska, L.; Scialis, R.; Zhang, H.; Umland, J.; et al. Quantitative Contribution of Six Major Transporters to the Hepatic Uptake of Drugs: "SLC-Phenotyping" Using Primary Human Hepatocytes. *J. Pharmacol. Exp. Ther.* **2019**, *370*, 72–83. [CrossRef] [PubMed]
58. Rowland, M.; Matin, S.B. Kinetics of drug-drug interactions. *J. Pharmacokinet. Biopharm.* **1973**, *1*, 553–567. [CrossRef]
59. Vieira, M.L.; Kirby, B.; Ragueneau-Majlessi, I.; Galetin, A.; Chien, J.Y.; Einolf, H.J.; Fahmi, O.A.; Fischer, V.; Fretland, A.; Grime, K.; et al. Evaluation of various static in vitro-in vivo extrapolation models for risk assessment of the CYP3A inhibition potential of an investigational drug. *Clin. Pharmacol. Ther.* **2014**, *95*, 189–198. [CrossRef]
60. Ohno, Y.; Hisaka, A.; Ueno, M.; Suzuki, H. General framework for the prediction of oral drug interactions caused by CYP3A4 induction from in vivo information. *Clin. Pharmacokinet.* **2008**, *47*, 669–680. [CrossRef]
61. Shou, M.; Hayashi, M.; Pan, Y.; Xu, Y.; Morrissey, K.; Xu, L.; Skiles, G.L. Modeling, prediction, and in vitro in vivo correlation of CYP3A4 induction. *Drug Metab. Dispos.* **2008**, *36*, 2355–2370. [CrossRef]
62. Bohnert, T.; Patel, A.; Templeton, I.; Chen, Y.; Lu, C.; Lai, G.; Leung, L.; Tse, S.; Einolf, H.J.; Wang, Y.; et al. Evaluation of a New Molecular Entity as a Victim of Metabolic Drug-Drug Interactions-an Industry Perspective. *Drug Metab. Dispos.* **2016**, *44*, 1399–1423. [CrossRef]
63. Obach, R.S. Predicting drug-drug interactions from in vitro drug metabolism data: Challenges and recent advances. *Curr. Opin. Drug Discov. Dev.* **2009**, *12*, 81–89.
64. Li, R.; Barton, H.A.; Varma, M.V. Prediction of pharmacokinetics and drug-drug interactions when hepatic transporters are involved. *Clin. Pharmacokinet.* **2014**, *53*, 659–678. [CrossRef]
65. Watanabe, T.; Kusuhara, H.; Maeda, K.; Kanamaru, H.; Saito, Y.; Hu, Z.; Sugiyama, Y. Investigation of the rate-determining process in the hepatic elimination of HMG-CoA reductase inhibitors in rats and humans. *Drug Metab. Dispos.* **2010**, *38*, 215–222. [CrossRef] [PubMed]
66. Varma, M.V.; Bi, Y.-a.; Kimoto, E.; Lin, J. Quantitative Prediction of Transporter- and Enzyme-Mediated Clinical Drug-Drug Interactions of Organic Anion-Transporting Polypeptide 1B1 Substrates Using a Mechanistic Net-Effect Model. *J. Pharmacol. Exp. Ther.* **2014**, *351*, 214–223. [CrossRef] [PubMed]
67. Varma, M.V.; Lin, J.; Bi, Y.A.; Kimoto, E.; Rodrigues, A.D. Quantitative Rationalization of Gemfibrozil Drug Interactions: Consideration of Transporters-Enzyme Interplay and the Role of Circulating Metabolite Gemfibrozil 1-O-beta-Glucuronide. *Drug Metab. Dispos.* **2015**, *43*, 1108–1118. [CrossRef] [PubMed]
68. Umehara, K.; Camenisch, G. Novel in vitro-in vivo extrapolation (IVIVE) method to predict hepatic organ clearance in rat. *Pharm. Res.* **2012**, *29*, 603–617. [CrossRef] [PubMed]
69. Varma, M.V.; Lin, J.; Bi, Y.A.; Rotter, C.J.; Fahmi, O.A.; Lam, J.L.; El-Kattan, A.F.; Goosen, T.C.; Lai, Y. Quantitative prediction of repaglinide-rifampicin complex drug interactions using dynamic and static mechanistic models: Delineating differential CYP3A4 induction and OATP1B1 inhibition potential of rifampicin. *Drug Metab. Dispos.* **2013**, *41*, 966–974. [CrossRef]
70. Rowland, M. Physiologically-Based Pharmacokinetic (PBPK) Modeling and Simulations Principles, Methods, and Applications in the Pharmaceutical Industry. *CPT Pharmacomet. Syst. Pharmacol.* **2013**, *2*, 55–56. [CrossRef]
71. Kuepfer, L.; Niederalt, C.; Wendl, T.; Schlender, J.F.; Willmann, S.; Lippert, J.; Block, M.; Eissing, T.; Teutonico, D. Applied Concepts in PBPK Modeling: How to Build a PBPK/PD Model. *CPT Pharmacomet. Syst. Pharmacol.* **2016**, *5*, 516–531. [CrossRef]

72. Jones, H.; Rowland-Yeo, K. Basic concepts in physiologically based pharmacokinetic modeling in drug discovery and development. *CPT Pharmacomet. Syst. Pharmacol.* **2013**, *2*, 63–74. [CrossRef]

73. Shin, H.K.; Kang, Y.M.; No, K.T. Predicting ADME properties of chemicals. In *Handbook of Computational Chemistry*, 2nd ed.; Leszczynski, J., Kaczmarek-Kedziera, A., Puzyn, T., Papadopoulos, M.G., Reis, H., Shukla, M.K., Eds.; Springer: Cham, Swizerland, 2017; Volume 59, pp. 2265–2301.

74. Yuan, D.; He, H.; Wu, Y.; Fan, J.; Cao, Y. Physiologically Based Pharmacokinetic Modeling of Nanoparticles. *J. Pharm. Sci.* **2019**, *108*, 58–72. [CrossRef]

75. El-Khateeb, E.; Burkhill, S.; Murby, S.; Amirat, H.; Rostami-Hodjegan, A.; Ahmad, A. Physiological-based pharmacokinetic modeling trends in pharmaceutical drug development over the last 20-years; In-depth analysis of applications, organizations, and platforms. *Biopharm. Drug Dispos.* **2020**. [CrossRef]

76. Zhang, X.; Yang, Y.; Grimstein, M.; Fan, J.; Grillo, J.A.; Huang, S.M.; Zhu, H.; Wang, Y. Application of PBPK Modeling and Simulation for Regulatory Decision Making and Its Impact on US Prescribing Information: An Update on the 2018-2019 Submissions to the US FDA's Office of Clinical Pharmacology. *J. Clin. Pharmacol.* **2020**, *60*, 160–178. [CrossRef]

77. Grimstein, M.; Yang, Y.; Zhang, X.; Grillo, J.; Huang, S.M.; Zineh, I.; Wang, Y. Physiologically Based Pharmacokinetic Modeling in Regulatory Science: An Update From the U.S. Food and Drug Administration's Office of Clinical Pharmacology. *J. Pharm. Sci.* **2019**, *108*, 21–25. [CrossRef] [PubMed]

78. Hartmanshenn, C.; Scherholz, M.; Androulakis, I.P. Physiologically-based pharmacokinetic models: Approaches for enabling personalized medicine. *J. Pharmacokinet. Pharmacodyn.* **2016**, *43*, 481–504. [CrossRef] [PubMed]

79. Rostami-Hodjegan, A. Physiologically based pharmacokinetics joined with in vitro-in vivo extrapolation of ADME: A marriage under the arch of systems pharmacology. *Clin. Pharmacol. Ther.* **2012**, *92*, 50–61. [CrossRef] [PubMed]

80. Tan, Y.M.; Chan, M.; Chukwudebe, A.; Domoradzki, J.; Fisher, J.; Hack, C.E.; Hinderliter, P.; Hirasawa, K.; Leonard, J.; Lumen, A.; et al. PBPK model reporting template for chemical risk assessment applications. *Regul. Toxicol. Pharmacol.* **2020**, *115*, 104691. [CrossRef] [PubMed]

81. Shebley, M.; Sandhu, P.; Emami Riedmaier, A.; Jamei, M.; Narayanan, R.; Patel, A.; Peters, S.A.; Reddy, V.P.; Zheng, M.; Zwart, L.; et al. Physiologically Based Pharmacokinetic Model Qualification and Reporting Procedures for Regulatory Submissions: A Consortium Perspective. *Clin. Pharmacol. Ther.* **2018**, *104*, 88–110. [CrossRef] [PubMed]

82. Asaumi, R.; Menzel, K.; Lee, W.; Nunoya, K.I.; Imawaka, H.; Kusuhara, H.; Sugiyama, Y. Expanded Physiologically-Based Pharmacokinetic Model of Rifampicin for Predicting Interactions With Drugs and an Endogenous Biomarker via Complex Mechanisms Including Organic Anion Transporting Polypeptide 1B Induction. *CPT Pharmacomet. Syst. Pharmacol.* **2019**, *8*, 845–857. [CrossRef]

83. Bayer Inc. Computational Systems Biology Suite. Available online: www.open-systems-pharmacology.org (accessed on 1 December 2020).

84. Simcyp Ltd. The Population-Based Simulator. Available online: www.simcyp.com (accessed on 1 December 2020).

85. Simulations Plus Inc. GastroPlus. Available online: www.simulations-plus.com (accessed on 1 December 2020).

86. Yamazaki, S.; Costales, C.; Lazzaro, S.; Eatemadpour, S.; Kimoto, E.; Varma, M.V. Physiologically-Based Pharmacokinetic Modeling Approach to Predict Rifampin-Mediated Intestinal P-Glycoprotein Induction. *CPT Pharmacomet. Syst. Pharmacol.* **2019**, *8*, 634–642. [CrossRef]

87. Rowland Yeo, K.; Jamei, M.; Yang, J.; Tucker, G.T.; Rostami-Hodjegan, A. Physiologically based mechanistic modelling to predict complex drug-drug interactions involving simultaneous competitive and time-dependent enzyme inhibition by parent compound and its metabolite in both liver and gut—The effect of diltiazem on the time-course of exposure to triazolam. *Eur. J. Pharm. Sci.* **2010**, *39*, 298–309.

88. Feng, B.; Varma, M.V. Evaluation and Quantitative Prediction of Renal Transporter-Mediated Drug-Drug Interactions. *J. Clin. Pharmacol.* **2016**, *56*, 110–121. [CrossRef]

89. Posada, M.M.; Bacon, J.A.; Schneck, K.B.; Tirona, R.G.; Kim, R.B.; Higgins, J.W.; Pak, Y.A.; Hall, S.D.; Hillgren, K.M. Prediction of renal transporter mediated drug-drug interactions for pemetrexed using physiologically based pharmacokinetic modeling. *Drug Metab. Dispos.* **2015**, *43*, 325–334. [CrossRef] [PubMed]

90. Watanabe, T.; Kusuhara, H.; Sugiyama, Y. Application of physiologically based pharmacokinetic modeling and clearance concept to drugs showing transporter-mediated distribution and clearance in humans. *J. Pharmacokinet. Pharmacodyn.* **2010**, *37*, 575–590. [CrossRef] [PubMed]

91. Rodrigues, A.D.; Taskar, K.S.; Kusuhara, H.; Sugiyama, Y. Endogenous Probes for Drug Transporters: Balancing Vision With Reality. *Clin. Pharmacol. Ther.* **2018**, *103*, 434–448. [CrossRef] [PubMed]

92. Guo, Y.; Chu, X.; Parrott, N.J.; Brouwer, K.L.R.; Hsu, V.; Nagar, S.; Matsson, P.; Sharma, P.; Snoeys, J.; Sugiyama, Y.; et al. Advancing Predictions of Tissue and Intracellular Drug Concentrations Using In Vitro, Imaging and Physiologically Based Pharmacokinetic Modeling Approaches. *Clin. Pharmacol. Ther.* **2018**, *104*, 865–889. [CrossRef] [PubMed]

93. Billington, S.; Shoner, S.; Lee, S.; Clark-Snustad, K.; Pennington, M.; Lewis, D.; Muzi, M.; Rene, S.; Lee, J.; Nguyen, T.B.; et al. Positron Emission Tomography Imaging of [^{11}C]Rosuvastatin Hepatic Concentrations and Hepatobiliary Transport in Humans in the Absence and Presence of Cyclosporin A. *Clin. Pharmacol. Ther.* **2019**, *106*, 1056–1066. [CrossRef] [PubMed]

94. Perry, C.; Davis, G.; Conner, T.M.; Zhang, T. Utilization of Physiologically Based Pharmacokinetic Modeling in Clinical Pharmacology and Therapeutics: An Overview. *Curr. Pharmacol. Rep.* **2020**, *6*, 71–84. [CrossRef] [PubMed]